In vivo behaviour of glyco-NaI@SWCNT 'nanobottles'

Sonia De Munari,[a] Stefania Sandoval,[b] Elzbieta Pach,[c] Belén Ballesteros,[c] Gerard Tobias,[b]*

Daniel C. Anthony[d]* and Benjamin G. Davis[a]*

[a]Chemistry Research Laboratory, Department of Chemistry, University of Oxford, Mansfield Road, Oxford OX1 3TA, UK

[b]Institut de Ciència de Materials de Barcelona (ICMAB-CSIC), 08193 Bellaterra, Barcelona, Spain

[c]Catalan Institute of Nanoscience and Nanotechnology (ICN2), CSIC and The Barcelona Institute of Science and Technology, Campus UAB, Bellaterra, 08193 Barcelona, Spain.

[d]Department of Pharmacology, University of Oxford, Mansfield Road, Oxford OX1 3QT, UK

* Corresponding authors.

E-mail addresses:

gerard.tobias@icmab.es

daniel.anthony@pharm.ox.ac.uk

ben.davis@chem.ox.ac.uk.

Abstract 212 words

Carbon nanotubes are appealing imaging and therapeutic systems. Their structure allows not only a useful display of molecules on their outer surface but at the same time the protection of encapsulated cargoes. Despite the interest they have provoked in the scientific community their applications have not yet been fully realised due to the limited knowledge we possess concerning their physiological behaviour. Previously, we have shown that the encapsulation of radionuclide in the inner space of glycan-functionalized single-walled carbon nanotubes (glyco-X@SWCNT) redirected *in vivo* distribution of radioactivity from the thyroid to the lungs. Here we test the roles played by such glycans attached to carbon nanotubes in controlling sites of accumulation using nanotubes carrying both 'cold' and 'hot' salt cargoes decorated with two different mammalian carbohydrates, *N*-acetyl-D-glucosamine (GlcNAc) or galactose(Gal)-capped disaccharide lactose (Gal–Glc). This distinct variation of the terminal glycan displayed between two types of glycan ligands with very different *in vivo* receptors, coupled with altered sites of administration, suggest that distribution in mammals is likely controlled by physiological mechanisms that may include accumulation in the first capillary bed they encounter and not by glycan-receptor interaction and that the primary role of glycan is in aiding the dispersibility of the CNTs.

Keywords: nanocrystals; nanocapsules; glycosylation; encapsulation; radioactive

1. Introduction

The inner cavities of carbon nanotubes (CNTs) can accommodate a wide range of guest species [1-4]. Unprecedented structures and properties compared to those of the same material in the bulk can be observed when they are confined [5-11]. In the biomedical field, contrast agents and therapeutic compounds can be either attached to the external CNT walls or confined within the cavities of the CNTs [12-18]. The latter is attractive because CNTs can offer striking protection to chosen payloads avoiding their interaction with the biological milieu [19].

Several strategies have been developed for the encapsulation of materials inside carbon nanotubes. Once filled, unless there is a strong interaction between the host nanotubes and the guest species, the ends of the CNTs need to be sealed/closed to allow selective purification from non-encapsulated materials left external to the CNT. Heating nanotubes together with inorganic salts at high temperatures allows capillary permeation of the melted salts inside the nanotubes with the spontaneous closure of the extremities during the cooling process [20, 21]. The salts remain stably confined in the form of ‘nanocrystals’ inside the nanotubes while leaving the outer surface unaffected, and so ready to be modified by organic molecules.

As-produced, CNTs are insoluble in almost any aqueous solution and organic solvent, and have been suggested to be toxic to mammalian cells [22], thereby presenting perceived limitations to their biological applications [23-27]. Functionalization of CNT side-walls with biologically- and biotechnologically- relevant molecules (including polymers [28], peptides [29, 30], nucleic acids [31] and carbohydrates [32, 33]) allows the generation of potentially stable and biocompatible dispersions. For example, non-covalent binding of aromatic molecules by π–π stacking onto the surface of the

nanotubes [34] or covalent modification of their polyarenic surface [35] allow efficient loading of multiple molecules along the length of the nanotubes.

We have previously shown that encapsulation of radionuclide into the inner space of glycan-functionalized single-walled carbon nanotubes (glyco-X@SWCNT) may be achieved by molten filling and then covalent modification, allowing *in vivo* redirection distribution of the associated radioactivity from the thyroid to the lungs.[33] Here, we use steam-purified and shortened single-walled carbon nanotubes (SWCNTs) [36] filled with both 'cold' (NaI) and 'hot' ($Na^{125}I$) cargoes and subsequent functionalization with different carbohydrates to explore the basis and role of glycan in this redistribution.

2. Experimental

2.1. Purification of SWCNTs

Chemical vapour deposition (CVD) grown SWCNTs, were provided by Thomas Swan & Co. Ltd (Elicarb®). Steam purification was carried out in order to remove the amorphous carbon and graphitic shells formed during the synthesis [36]. Steam treatment was simultaneously employed to open the SWCNTs ends. For this purpose, 1 g of as-received SWCNTs were ground with agate mortar and pestle and then placed inside a tubular furnace. Steam was introduced by bubbling argon through hot water. The temperature was raised by 20 °C/min till 900 °C, where the SWCNTs remained for 25 h. After cooling at a rate of 10 °C/min down to 25 °C, the powder was dispersed in a 6 M HCl solution and refluxed at 110 °C during 6 h to remove the iron catalyst exposed after the steam oxidation of the graphitic shells. The mixture was cooled, filtered using a 0.2 μm polycarbonate membrane, washed with distilled water until neutral pH was reached and dried overnight at 60 °C. After this treatment, SWCNTs with a median length of ca. 200 nm are obtained [37].

2.2. Filling of SWCNTs with NaI by molten phase capillary wetting

Purified and open-ended SWCNTs (100 mg) and NaI (1 g) were ground together and loaded into a silica ampoule. The system was evacuated and the ampoule was sealed under vacuum. The sample was subsequently annealed at 900 °C and slowly cooled down to favour the crystallization of NaI within the hosting SWCNTs. Afterwards, the system was air opened and the sample was ground with an agate mortar and pestle. The sample was next washed in water, to remove the non-encapsulated NaI, and collected by filtration on top of a polycarbonate membrane (0.2 μm Whatman).

2.3. Synthesis of f-NaI@SWCNTs

4-(2-(bis(2-tert-butoxycarbonyl-aminoethyl)amino)ethylamino)oxobutanoic acid: To a solution of tris(2-aminoethyl)amine (6 mL, 41 mmol, 5 eq.) in ACN (200 mL) at 0 °C was added, dropwise, a solution of succinic anhydride (822 mg, 8.2 mmol, 1 eq.) in ACN (100 mL). The reaction was stirred at r.t. for 2 h, before the solution was poured away and the precipitate recovered with MeOH, and finally dried under vacuum to afford 4-(2-(bis(2-aminoethyl)amino)ethylamino)oxobutanoic acid as a yellow oil (2.0 g, 8 mmol, 98%).

To a solution of 4-(2-(bis(2-aminoethyl)amino)ethylamino)oxobutanoic acid (343 mg, 1.39 mmol, 1 eq.) in dioxane (15 mL) was added di-*tert*-butyl dicarbonate (611 mg, 2.8 mmol, 2 eq.). The reaction mixture was stirred for 4 h at r.t. The reaction was evaporated, and the residue purified by flash column chromatography over silica (DCM:MeOH, 10:0.2 to 10:2), to afford the title compound as a white solid (246.8 mg, 0.55 mmol, 40%).

N-(2,2'-(ethylenedioxy)diethylamino) benzylacetate: To a solution of N-(N-*tert*-butoxycarbonyl-(2,2'-(ethylenedioxy)diethylamino)) benzylacetate [38] (1.1056 g, 2.79 mmol, 1 eq.) in DCM (5.6 mL) was added TFA (2.4 mL). The reaction was stirred at r.t. for 1

h, before being evaporated under vacuum to afford the title compound as a yellow oil (1.08 g, 2.79 mmol, quant.).

*N-(4-(2-(bis(2-tert-butoxycarbonyl-aminoethyl)amino)ethylamino)oxobutanoyl) N-(2,2'-ethylenedioxy)diethylamino)benzylic acid (***1.0***):*

(1) To a solution of 4-(2-(bis(2-*tert*-butoxycarbonyl-aminoethyl)amino)ethylamino) oxobutanoic acid (1.230 g, 2.75 mmol, 1 eq.) in DMF (55 mL), were added HATU (2.091 g, 5.5 mmol, 2 eq.), HOBt (743 mg, 5.5 mmol, 2 eq.) and DIPEA (960 µL, 5.5 mmol, 2 eq.). Finally, N-(2,2'-(ethylenedioxy)diethylamino) benzylacetate (978.8 mg, 3.3 mmol, 1.2 eq.) was added and the mixture stirred at r.t. for 6 h. The reaction was evaporated to a small volume, recovered with DCM (150 mL) and washed with H_2O (200 mL) and Brine (200 mL). The organic layer was dried over $MgSO_4$ and evaporated under vacuum, to afford the title compound as a yellow oil (1.8455 g, 2.55 mmol, 92%).

(2) To Pd/C (10 mg, 10 wt. % loading) under hydrogen, was added a solution of N-(4-(2-(bis(2-*tert*-butoxycarbonyl-aminoethyl)amino)ethylamino)oxobutanoyl) N-(2,2'-ethylenedioxy) diethylamino) benzylacetate (386 mg, 0.53 mmol, 1 eq.) in MeOH (dry, 3 mL). The reaction mixture was stirred at r.t. for 5 h, filtered over celite and evaporated under vacuum. The crude was purified by flash column chromatography on silica (DCM:MeOH, 9:1 to 0:1) to afford the title compound as a colourless oil (220.4 mg, 0.35 mmol, 66%).

A suspension of NaI@SWCNTs (6 mg) in DMF (dry, 3 mL) was sonicated for 2 min, before a solution of N-(4-(2-(bis(2-*tert*-butoxycarbonyl-aminoethyl)amino)ethylamino)oxobutanoyl) N-(2,2'-ethylenedioxy)diethylamino)benzylic acid **1.0** (12.7 mg, 0.02 mmol, 1 eq.) and 2,3,5-triiodobenzaldehyde [33] (9.6 mg, 0.02 mmol, 1 eq.) in DMF (dry, 1 mL) was added. The

reaction was refluxed at 130 °C for 4 days, then cooled to r.t. and filtered. The solid was washed with DMF, MeOH and dried under vacuum to afford di-Boc-*f*-NaI@SWCNTs as a black solid (6.8 mg).

A suspension of di-Boc-*f*-NaI@SWCNTs (12.2 mg) in DCM (dry, 5 mL) was sonicated for 2 min, before TFA (2.5 mL) was added. The reaction was stirred at r.t. for 24 h, then evaporated, recovered with MeOH, filtered and washed with MeOH. The solid obtained was dried under vacuum to afford the title compound as a black solid (9.46 mg).

2.4. Fmoc numbering *f*-NaI@SWCNTs

A solution of Fmoc chloride (1 mg, 3.86 μmol, 1 eq.) in DCM (0.5 mL) was added dropwise to a suspension of *f*-NaI@SWCNTs (1 mg) in DCM (0.5 mL) at 0 °C. DIPEA (1.5 μL, 8.61 μmol, 2.2 eq.) was added and the reaction was stirred at r.t. for 16 h. The reaction mixture was centrifuged, the supernatant discarded and the solid recovered with MeOH then filtered and washed with MeOH. The solid obtained was dried under vacuum and treated with DMSO:DMF:DBU (25:24:1 solution, 1 mL) at r.t. to cleave the Fmoc group. After 2 h, 20 μL of the crude were added to 1000 μL of MeOH. The sample was centrifuged and the absorbance of the solution measured by UV at 295 nm (A = 0.065698, Ɛ = 10,027 $cm^{-1}M^{-1}$). The functionalization of the nanotubes obtained was 0.34 mmol/g.

2.5 Synthesis of Glycosylated-NaI@SWCNTs

2-acetamido-1-thio-(S-2-imido-2-methoxyethyl)-2-deoxy-β-D-glucopyranoside **1.1***:* To a solution of 2-N-acetamido-3,4,6-tri-O-acetyl-2-deoxy-1-thio-(S-cyanomethyl)-β-D-glucopyranoside [39] (20 mg, 0.05 mmol, 1 eq.) in MeOH (dry, 1 mL) was added NaOMe (25% in MeOH, 12 μL, 0.05 mmol, 1 eq.). The reaction was stirred at r.t. for 16 h before

being neutralised with DowexH^+. The reaction mixture was filtered and evaporated without heating. The product was obtained as a mixture of deprotected (R-SCM) and activated sugars (R-IME, **2.80**) in ratio 1:0.5 (determined by NMR, ^{1}H, MeOD), and used in the next step without further purification.

2,3,6-O-tri-O-acetyl-4-O-[2,3,4,6-tetra-O-acetyl-β-D-galactopyranosyl]-1-thio-(S-cyanomethyl)-β-D-glucopyranoside To β-lactose (10 g, 29.2 mmol, 1 eq.) were added Ac_2O (155 mL, 1636 mmol, 56 eq.) and NaOAc (10 g, 122.6 mmol, 4.2 eq.). The reaction was stirred at 140 °C for 5 h, recovered with H_2O (200 mL) and extracted with DCM (3 x 200 mL). The organic layer was washed with $NaHCO_3$ satd. solution (200 mL) and brine (200 mL), then dried over $MgSO_4$, evaporated and co-evaporated with toluene, to afford 1,2,3,6-O-tetra-O-acetyl-4-O-[2,3,4,6-tetra-O-acetyl-β-D-galactopyranosyl]-β-D-glucopyranoside [40] as a light yellow foam (19.9 g, 29.2 mmol, quant.).

To 1,2,3,6-O-tetra-O-acetyl-4-O-[2,3,4,6-tetra-O-acetyl-β-D-galactopyranosyl]-β-D-glucopyranoside (14.15 g, 20.85 mmol, 1 eq.) in an ice bath, were added HBr (33% in AcOH, 23 mL, 129.27 mmol, 6.2 eq.) and Ac_2O (4.2 mL, 43.785 mmol, 2.1 eq.). The reaction was stirred for 3 h, recovered with DCM (200 mL) and poured into H_2O (200 mL). The mixture was stirred with $NaHCO_3$ satd. solution (300 mL), the organic layer separated and washed with $NaHCO_3$ satd. solution (3 x 200 mL) and brine (200 mL). The organic layer was dried over $MgSO_4$ and evaporated to afford 2,3,6-O-tri-O-acetyl-4-O-[2,3,4,6-tetra-O-acetyl-β-D-galactopyranosyl]-1-bromo-α-D-glucopyranoside [41] as a white foam (13.27 g, 19 mmol, 91%).

2,3,6-O-tri-O-acetyl-4-O-[2,3,4,6-tetra-O-acetyl-β-D-galactopyranosyl]-1-bromo-α-D-glucopyranoside (14.58 g, 20.85 mmol, 1 eq.) was mixed with thiourea (3.5 g, 45.87 mmol,

2.2 eq.) and dissolved in acetone (50 mL). The reaction was stirred for 3 h at 80 °C, then evaporated. The solid was recovered with acetone (60 mL), and $Na_2S_2O_5$ (10.3 g, 54.21 mmol, 2.6 eq.), K_2CO_3 (4 g, 29.19 mmol, 1.4 eq.) and chloroacetonitrile (20 mL, 316.92 mmol, 15.2 eq.) were added The mixture was stirred at r.t. for 3 h, evaporated and purified by flash column chromatography on silica (EtOAc:PE, 1:1) to afford the title compound as a white foam (8.7621 g, 12.6 mmol, 63%).

4-O-[β-D-galactopyranosyl]-1-thio-(S-2-imido-2-methoxyethyl)-β-D-glucopyranoside **1.2***:* To a solution of 2,3,6-O-tri-O-acetyl-4-O-[2,3,4,6-tetra-O-acetyl-β-D-galactopyranosyl]-1-thio-(S-cyanomethyl)-β-D-glucopyranoside (100 mg, 0.14 mmol, 1 eq.) in MeOH (dry, 1 mL) was added NaOMe (25% in MeOH, 33 µL, 0.14 mmol, 1 eq.). The reaction was stirred at r.t. for 16 h before being neutralised with DowexH$^+$. The reaction mixture was filtered and evaporated without heating. The product was obtained as a mixture of deprotected (R-SCM) and activated sugars (R-IME, **2.87**) in ratio 1:0.7 (determined by NMR, ^{1}H, MeOD), and used in the next step without further purification.

GlcNAc-NaI@SWCNTs: A solution of 2-acetamido-1-thio-(S-2-imido-2-methoxyethyl)-2-deoxy-β-D-glucopyranoside (6.5 mg, 20 µmol, 1 eq.) in MeOH:DMSO (2:1, 1.5 mL) was added to a suspension of *f*-NaI@SWCNTs (1 mg) in DCM (0.5 mL). The reaction was stirred at r.t. for 30 min. The reaction mixture was centrifuged, the supernatant discarded and the solid recovered with MeOH, filtered and washed with MeOH. The solid obtained was dried under vacuum to afford the title compound as a black solid (0.88 mg). **EA** (C, H, N) 67.34, 1.08, 2.98.

Lac-NaI@SWCNTs: A solution of 4-O-[β-D-galactopyranosyl]-1-thio-(S-2-imido-2-methoxyethyl)-β-D-glucopyranoside (6.5 mg, 20 µmol, 1 eq.) in MeOH:DMSO (2:1, 1.5 mL) was added to a suspension of *f*-NaI@SWCNTs (1 mg) in DCM (0.5 mL). The reaction was

stirred at r.t. for 30 min. The reaction mixture was centrifuged, the supernatant discarded and the solid recovered with MeOH, filtered and washed with MeOH. The solid obtained was dried under vacuum to afford the title compound as a black solid (0.8 mg). **EA** (C, H, N) 67.32 ,1.11, 3.01.

2.6 Synthesis of glycosylated-Na^{125}I@SWCNTs

Filling of SWCNTs with Na^{125}I: Steam-purified SWCNTs (1 mg) were loaded in a silica ampoule with Na^{125}I solution (10^{-5} M, 100 µL, 20 MBq), dried and sealed under high vacuum with an oxygen-propane flame. The ampoule was heated in a furnace up to 900 °C using the same ramp described for the cold samples. The sample was recovered from the ampoule with H_2O (1 mL), sonicated and filtered. Final activity = 9 MBq (1 mg, RCY = 45%).

f-Na^{125}I@SWCNTs: A suspension of Na^{125}I@SWCNTs (1 mg, 9 MBq) in DMF (dry, 3 mL) was sonicated for 2 min, before a solution of N-(4-(2-(bis(2-*tert*-butoxycarbonyl-aminoethyl)amino)ethylamino) oxobutanoyl) N-(2,2'-ethylenedioxy)diethylamino)benzylic acid (12.7 mg, 0.02 mmol, 1 eq.) and 2,3,5-triiodobenzaldehyde (9.6 mg, 0.02 mmol, 1 eq.) in DMF (dry, 1 mL) was added. The reaction was refluxed at 130 °C for 4 days, then cooled to r.t. and filtered. The solid was washed with DMF, MeOH and dried under vacuum to afford di-Boc-*f*-Na^{125}I@SWCNTs as a black solid (1 mg, 9 MBq).

A suspension of di-Boc-*f*-Na^{125}I@SWCNTs (1 mg, 9 MBq) in DCM (dry, 5 mL) was sonicated for 2 min, before TFA (2.5 mL) was added. The reaction was stirred at r.t. for 24 h, then evaporated, recovered with MeOH, filtered and washed with MeOH. The solid obtained was dried under vacuum to afford the title compound *f*-Na^{125}I@SWCNTs as a black solid (1 mg, 9 MBq).

GlcNAc-Na^{125}I@SWCNTs: A solution of 2-acetamido-1-thio-(S-2-imido-2-methoxyethyl)-2-deoxy-β-D-glucopyranoside (6.5 mg, 20 μmol, 1 eq.) in MeOH:DMSO (2:1, 1.5 mL) was added to a suspension of *f*-Na^{125}I@SWCNTs (0.3 mg, 3 MBq) in DCM (0.5 mL). The reaction was stirred at r.t. for 30 min. The reaction mixture was centrifuged, the supernatant discarded and the solid recovered with MeOH, filtered and washed with MeOH. The solid obtained was dried under vacuum to afford the title compound as a black solid (0.3 mg, 3 MBq).

Lac-Na^{125}I@SWCNTs: A solution of 4-O-[β-D-galactopyranosyl]-1-thio-(S-2-imido-2-methoxyethyl)-β-D-glucopyranoside (6.0 mg, 20 μmol, 1 eq.) in MeOH:DMSO (2:1, 1.5 mL) was added to a suspension of Na^{125}I@SWCNTs (0.3 mg, 3 MBq) in DCM (0.5 mL). The reaction was stirred at r.t. for 30 min. The reaction mixture was centrifuged, the supernatant discarded and the solid recovered with MeOH, filtered and washed with MeOH. The solid obtained was dried under vacuum to afford the title compound as a black solid (0.3 mg, 3 MBq).

For characterization details, namely, TGA, HRTEM, STEM, TLC, NMR mass spectrometry and Infrared spectroscopy see Supporting information.

3. Results and discussion

3.1 Preparation of 'cold' glyco-NaI@SWCNTs.

To prepare the nanotubes for filling they were first treated with steam, followed by an HCl (aq) wash, in order to remove graphitic nanoparticles, amorphous carbon and metal catalysts that remain as impurities from their generation [36]. This method also results in simultaneous shortening of the nanotubes *via* a process believed to involve oxidation and

decarboxylation of more reactive carbon atoms present at their tips [36]. TEM images of both as-received and steam-purified SWCNTs are shown in **Figure S1**; these revealed some residual iron-derived nanoparticles (from the preparative catalyst) after steam treatment. Sodium iodide (hot or cold) was filled into these carbon nanotubes to generate NaI@SWCNTs by adaptation of the protocol developed by Green *et al.* for the creation of KI 'nanocrystals' in SWCNTs [5]. Thus, a mixture of steam purified SWCNTs and the metal halide was annealed above the melting point of the inorganic salt ($m.p._{NaI}$ = 661 ºC) inside an evacuated silica ampoule. Heating at 900 ºC not only drove encapsulation of salt inside the nanotubes, but also induced the closing of their tips [20]. In this way, internal NaI crystals were isolated from the outer environment by the formation of carbon 'nanocapsules' [42] (or 'nanobottles' [30]). As a result, any residual, external NaI present after synthesis was easily removed simply by washing the sample in refluxing water.

Characterization by high-angle annular dark-field scanning transmission electron microscopy (HAADF-STEM) allowed encapsulated salt to be clearly discerned from the walls of the nanotubes (**Figure 1**). Visual inspection allowed filled SWCNTs containing heavy atoms (**Figure S2**, white arrowed) to be readily distinguished from empty (red arrowed). This also confirmed that washing with water after filling successfully removed all residual salt from the outer surfaces of the CNTs in the sample. Successful encapsulation of NaI was also confirmed using high-resolution transmission electron microscopy (HRTEM, **Figure 1b**), allowing observation of even the crystalline lattice of encapsulated NaI. Finally, analysis of the sample with energy dispersive X-ray spectroscopy (EDX, **Figure 1c**) further confirmed the presence of Na and I within the encapsulated cargo.

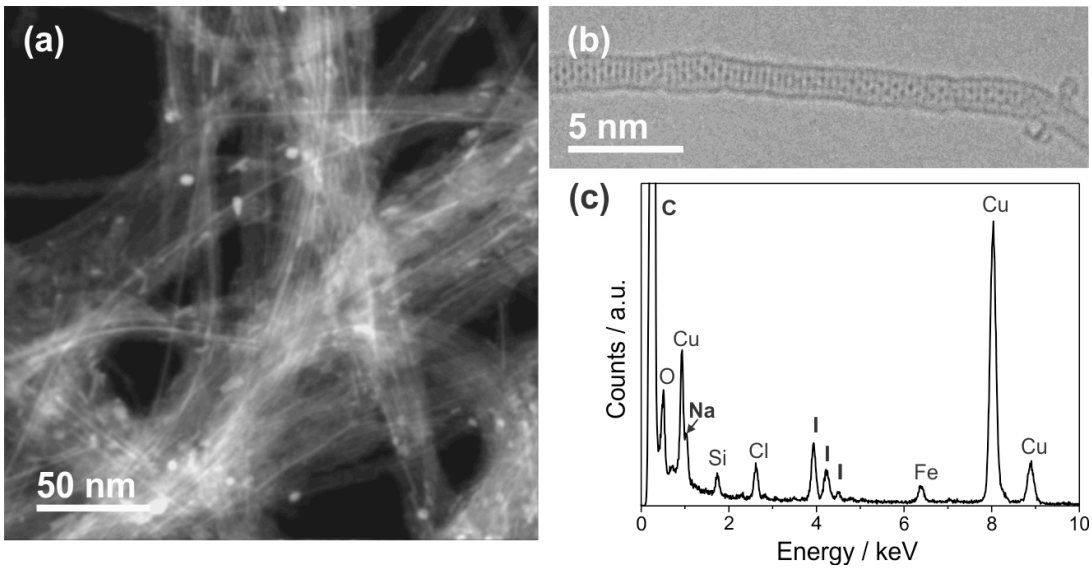

Fig. 1. NaI-filled SWCNTs (NaI@SWCNT). (**a**) HAADF-STEM; since the intensity of the signal scales up to *ca* the square of the atomic number, the heavier atoms of the guest (Na and I) appear as brighter lines along the inner cavities of the nanotubes compared to C from their walls; (**b**) HRTEM image; (**c**) EDX spectroscopy confirmed the presence of Na and I. Fe and Cu signals correspond to those from SWCNT-generation catalyst residuals and the copper grid used for supporting the sample, respectively. Si signal arises from the EDX detector.

Following successful filling to form NaI@SWCNT, covalent functionalization of the sidewalls was achieved under mild conditions via 1,3-dipolar cycloaddition using appropriately functionalized azomethine ylids [14, 43, 44] (**Scheme 1**). The choice of ylid also simultaneously allowed introduction of a 2,3,5-triiodophenyl motif as a 'marker' or 'tagging' motif,[45] suitable for the ready detection of successful functionalization using electron microscopy. To allow more ready diversification of glycan, a prior strategy devised by Hong *et al.* [33] was altered through first introducing a Boc-protected *bis*-amine branched linker moiety **1.0** to the CNT (**Scheme 1**), followed by deprotection using TFA to form a functionalized divergent intermediate, *f*-NaI@SWCNT. Fmoc-numbering[33] was employed to quantify the loading of the primary amine groups thus introduced and hence the degree of functionalization at 0.34 mmol/g.

Intermediate *f*-NaI@SWCNT was then subsequently glycoconjugated with appropriate amine-reactive glycan-IME imidate reagents,[46, 47] GlcNAc-IME **1.1** or Lac-IME **1.2** to introduce GlcNAc or lactose (Galβ1,4–Glc) to the linkers attached to surface of the NaI@SWCNT, respectively, forming $[GlcNAc]_2$-NaI@SWCNT or $[Lac]_2$-NaI@SWCNT (**Scheme 1**).

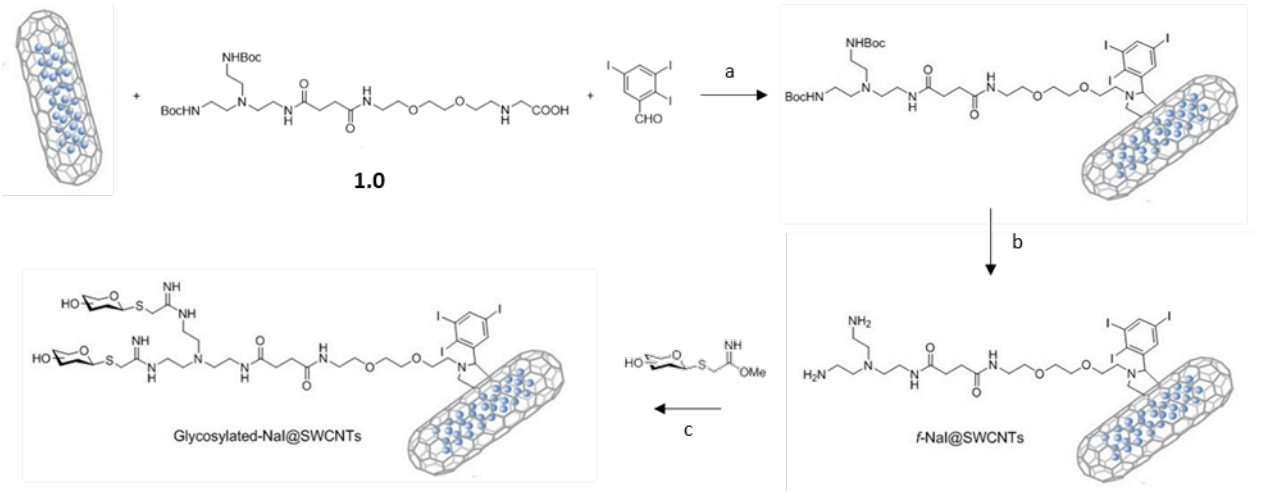

Scheme 1. Functionalization of NaI@SWCNTs with biantennary linker reagent **1.0** and subsequent glycosylation. Reagents and conditions: a) DMF, 130 °C, 4 days; b) DCM, TFA, r.t., 24h; c) MeOH:DMSO (2:1), r.t., 30 min.

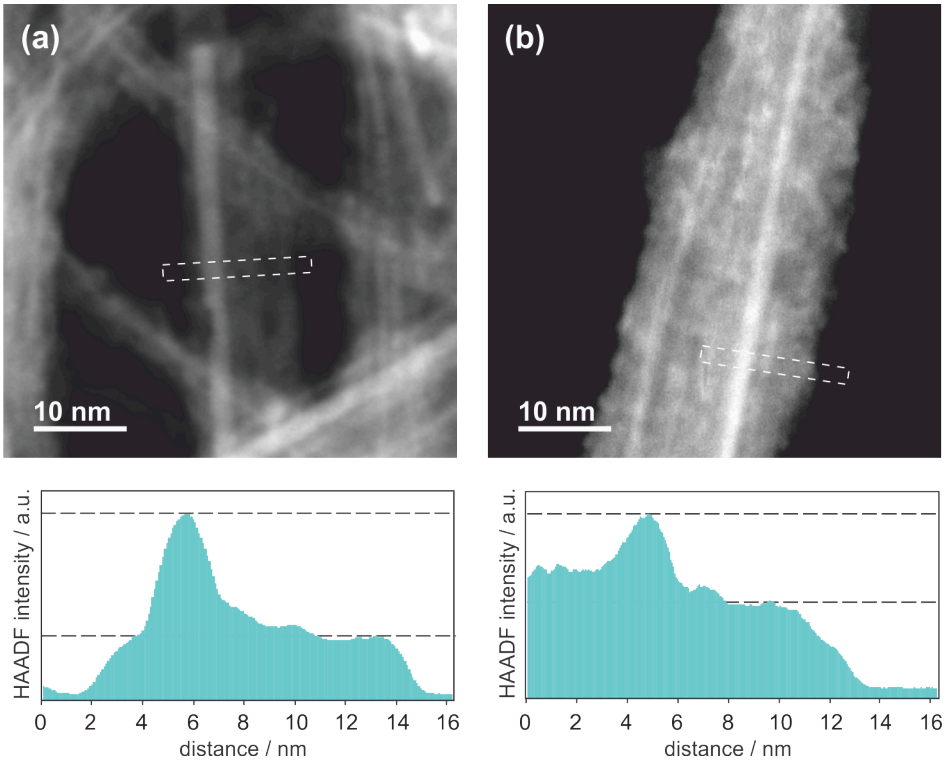

Fig. 2. HAADF-STEM images of (**a**) as-filled sample and (**b**) after GlcNAc functionalization to form $[GlcNAc]_2$-NaI@SWCNT. The respective HAADF intensity profiles along the white dashed boxes demonstrate that the intensity in the bundle area is higher for the $[GlcNAc]_2$-NaI@SWCNT, in agreement with the presence of iodide (*Z* = 53) in surface functional groups that have a substantial contribution to the signal.

HAADF-STEM imaging of the samples after GlcNAc functionalization **Figure 2** revealed a higher intensity in the bundle area when compared to the as-filled NaI@SWCNTs, due to the presence of the 2,3,5-triiodophenyl 'marker' combined into the linker moiety, thereby confirming successful covalent functionalization. The introduction of the linker to the surface of NaI@SWCNTs in *f*-NaI@SWCNTs, $[GlcNAc]_2$-NaI@SWCNT and $[Lac]_2$-NaI@SWCNT was also confirmed by TGA (**Figure 3**). Unlike the NaI@SWCNTs whose combustion starts ~ 400 ºC, weight loss at lower temperatures even down to ~ 200 ºC was observed that can be attributed to the combustion of the organic fraction attached to the nanotubes. GlcNAc and Lac functionalized SWCNTs showed higher thermal stabilities than the linker-functionalized SWCNT f-NaI@SWCNTs. During functionalization inorganic materials are employed (e.g. $MgSO_4$) that appear to remain in the functionalized samples and contribute to an unexpected increase in the amount of inorganic residue collected after the TGA for those samples that have been through these processes (**SI Figure S4**). Successful glycoconjugation was further confirmed by elemental combustion analyses (see Supplementary Information).

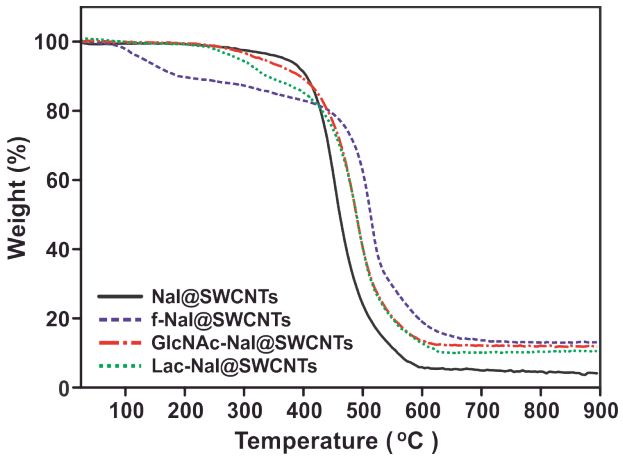

Fig. 3. TGA analyses of NaI filled SWCNTs (NaI@SWCNTs), and after being externally functionalized (f-NaI@SWCNTs) and glycosylated ($[GlcNAc]_2$-NaI@SWCNTs and $[Lac]_2$-NaI@SWCNTs).

3.2 Preparation of 'hot' glyco-Na^{125}I@SWCNTs.

One mode in which glycosylated-'nanocapsules/bottle' might be exploited is in the highly controlled and localized delivery of radioactivity. This also potentially allows quantification of biodistribution and even direct imaging of this delivery. To test the potential of our glycosylated nanotubes *in vivo* we created 'hot nanobottle' isotopologue variants in which we replaced 'cold' NaI with 'hot', radioactive Na^{125}I. Gamma emission from ^{125}I allows sensitive quantification and hence whole body distribution of constructs through 'gamma counting' of samples. Empty SWCNTs underwent an adapted molten phase filling process: SWCNTs and an aqueous solution of the radioactive salt were placed in a silica ampoule and heated to remove water. The ampoule was then sealed under vacuum and annealed following the protocol employed for 'cold' NaI. The functionalization and glycoconjugation process was carried out in an essentially analogous manner to that used for non-radioactive samples to generate 'hot' *f*-Na^{125}I@SWCNTs (0.3 mg, 3 MBq), 'hot' [GlcNAc]$_2$-Na^{125}I@SWCNTs (0.3 mg, 3 MBq) and 'hot' [Lac]$_2$-Na^{125}I@SWCNTs (0.3 mg, 3 MBq).

3.3 Biodistribution analyses of 'hot' and 'cold' glyco-NaI@SWCNTs.

Previous studies performed on the robustness of radionuclide-filled nanotubes in biological environments have shown a strong correlation between radioactivity and nanotube distribution, suggesting negligible leakage of radionuclide salts [33, 48]. This is particularly the case when using radio-iodide as 'cargo'; free iodide is readily taken up by the thyroid leading to sensitive observation – no such free iodide was detected in these prior studies. We used this correlation to quantify the distribution of nanotubes via gamma emission from the encapsulated Na^{125}I cargo. 'Hot' glyco-Na^{125}I@SWCNTs

were injected in CD-1 male mice (0.1 mg/100 μL) and biodistribution after 1 hour determined from gamma radiation levels in different organs (lungs, liver, spleen, brain, gut, kidneys, muscle and heart) *ex vivo* (**Figure 4**).

Two variants of mammalian glycans were chosen to test influence upon biodistribution. Both have putative endogenous receptors in mammals with different *in vivo* distribution. GlcNAc was used in our prior study in which functionalized NaI@SWCNTs containing radioactive iodide was successfully delivered into the lungs [33] and was again used here in $[GlcNAc]_2$-$Na^{125}I$@SWCNT. Galactosyl-terminated, Lac, is considered to be a 'liver-targeting' agent due to its interaction as a ligand with the asialoglycoprotein receptors expressed on hepatocytes [49] and was selected in this study as the second glycan and used in $[Lac]_2$-$Na^{125}I$@SWCNT. The distribution profile determined from both $[GlcNAc]_2$-$Na^{125}I$@SWCNT and $[Lac]_2$-$Na^{125}I$@SWCNT (**Figure 4**), however, showed no significant differences in biodistribution with essentially complete accumulation of the radioactivity in the lungs for both samples after tail-vein injection. This negligible influence of glycan was further confirmed by the identical *in vivo* behaviour of non-glycosylated precursor *f*-$Na^{125}I$@SWCNT (**Figure 4**).

Next, in order to test whether biodistribution could be attributed to dominant, inherent physiological properties of the nanotubes, we attempted to assess the effect of an alternative injection site *via* intra-aortic injection that necessitated preferential use of 'cold' glyco-SWCNTs and quantification instead by ICP-MS of tissue-derived samples. These analyses calibrated by internal standard revealed a lower method detection limit for iodide in tissue under these conditions of ~25 ng/g.tissue; iodide was also successfully observed in samples from animals treated with glyco-NaI@SWCNT at levels of up to 126 ng/g.tissue. However, although iodide levels were found in certain organs (liver, lung and spleen) of up to 60 ng/g.tissue above those found in control,

untreated animals, these should be treated as only suggestive *qualitative* indications – statistical analyses do not allow support of any quantitative significance. Thus, whilst these *may* be indicative of broader organ distribution caused by an alternative injection site, the use of 'cold iodide' tracking of filled, functionalized NaI@SWCN *in vivo* by ICP-MS analysis of tissues appears to lack the sensitivity required for unambiguous biodistribution analysis.

Together these data suggested that, at the loadings of surface functionalization used here, glycosylation serves only to aid dispersibility rather than providing any form of 'targeting'. Instead, once dispersed, glyco-SWCNTs may deliver their 'cargo' via various physiological mechanisms that may include recruitment at the first capillary bed that they encounter after *i.v.* administration, e.g. tail→lung.

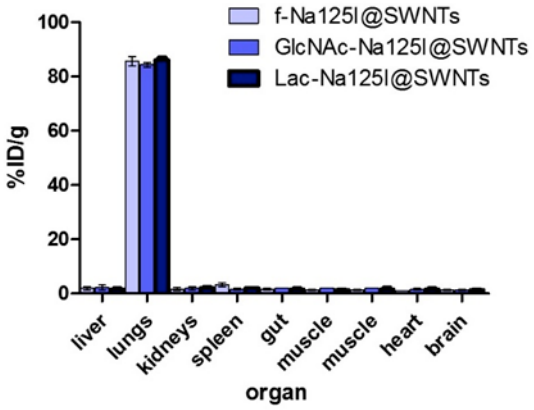

Fig. 4. Biodistribution of amine-functionalized and glycosylated $Na^{125}I$@SWCNTs. Organs of CD-1 mice were harvested 1 h after tail-vein injection of amine-functionalized (f-$Na^{125}I$@SWCNTs) and glycosylated nanotubes (GlcNAc-$Na^{125}I$@SWCNTs; Lac-$Na^{125}I$@SWCNTs). The distribution of the samples in the tissues was determined by ɣ-counting and expressed as percentage of the injected dose per g of tissue (%ID/g).

4. Conclusions

Functionalized and glycosylated nanotubes can act as ‘nanocapsules’ or ‘nanobottles’ to redirect the accumulation of inorganic radionuclide ‘cargo’ concealed in their inner void (here iodide) from a natural physiological target (here thyroid) [50] to alternative targets. At the functionalization loadings used here, different glycosylation patterns on these glyco-‘nanobottle’ constructs did not modulate *in vivo* distribution profiles. Instead, these appear to only aid dispersibility; these dispersed carbon nanotubes then appear to accumulate in a manner that is primarily determined by their physical properties within physiology (e.g. recruitment at the first capillary bed that they encounter) in a manner that is more likely to be determined by administration site than by any specific ligand-receptor targeting interaction at these lower loading of surface ligands on filled SWCNTs. It should be noted that overly high rates of injection can affect distribution. We injected 100μL of suspension over a 10-second period in which the heart would normally pump ~2.5-3.0 mL of blood. The mouse has a blood volume of ~1.5mL. Thus our injection was less than 4% volume at a rate well below suggested typical maximum of, e.g. 50 μL/s.{Diehl, 2001 #79}

These ‘nanocapsules/bottles’ may represent a useful, sealed ‘source of radiation’. If this could be combined with the benefits of a deliverable system, this could create a potentially suitable form of ‘nanobrachytherapy’. Given the seemingly dominant control of physical properties rather than biochemical properties upon distribution observed here, we speculate that future manipulation of not only surface functionalization (e.g. at higher levels or with different types) but even via changes to carbon nanostructure at a SWCNT level might usefully influence their *in vivo* capabilities.

Acknowledgements

This works was supported by EU FP7-ITN Marie-Curie Network programme RADDEL [grant number 290023] and the EU FP7-Integrated Infrastructure Initiative–I3 programme ESTEEM2 [grant number 312483]. We acknowledge financial support from Spanish Ministry of Economy and Competitiveness through the “Severo Ochoa” Programme for Centres of Excellence in R&D [grant numbers SEV-2015-0496, ICMAB; SEV-2017-0706, ICN2]. The ICN2 is funded by the CERCA programme. We would like to thank Thomas Swan & Co. Ltd. for supplying Elicarb® SWNT.

Finally and above all, this work on probing the potential of such ‘nanobottles’ in physiology has been inspired by many stimulating and fruitful conversations with Prof Malcolm Green – his insight and vision, as on many occasions, has proven invaluable.

Appendix A. Supplementary data

References

[1] J. Sloan, A.I. Kirkland, J.L. Hutchison, M.L.H. Green, Chem. Commun., (2002) 1319-1332.
[2] M. Monthioux, E. Flahaut, Mater. Sci. Eng. C, 27 (2007) 1096-1101.
[3] U.K. Gautam, P.M.F.J. Costa, Y. Bando, X. Fang, L. Li, M. Imura, D. Golberg, Sci. Technol. Adv. Mater., 11 (2010) 054501.
[4] A.N. Khlobystov, ACS Nano, 5 (2011) 9306-9312.
[5] R.R. Meyer, J. Sloan, R.E. Dunin-Borkowski, A.I. Kirkland, M.C. Novotny, S.R. Bailey, J.L. Hutchison, M.L.H. Green, Science, 289 (2000) 1324-1326.
[6] E. Philp, J. Sloan, A.I. Kirkland, R.R. Meyer, S. Friedrichs, J.L. Hutchison, M.L.H. Green, Nat. Mater., 2 (2003) 788.
[7] D.G. Calatayud, H. Ge, N. Kuganathan, V. Mirabello, R.M.J. Jacobs, N.H. Rees, C.T. Stoppiello, A.N. Khlobystov, R.M. Tyrrell, E.D. Como, S.I. Pascu, ChemistryOpen, 7 (2018) 144-158.
[8] A. Vasylenko, S. Marks, J.M. Wynn, P.V.C. Medeiros, Q.M. Ramasse, A.J. Morris, J. Sloan, D. Quigley, ACS Nano, 12 (2018) 6023-6031.
[9] L. Cabana, B. Ballesteros, E. Batista, C. Magén, R. Arenal, J. Oró-Solé, R. Rurali, G. Tobias, Adv. Mater., 26 (2014) 2016-2021.
[10] M. Hart, J. Chen, A. Michaelides, A. Sella, M.S.P. Shaffer, C.G. Salzmann, Angew. Chem. Int. Edit., 57 (2018) 11649-11653.
[11] S. Sandoval, D. Kepić, Á. Pérez del Pino, E. György, A. Gómez, M. Pfannmoeller, G.V. Tendeloo, B. Ballesteros, G. Tobias, ACS Nano, 12 (2018) 6648-6656.

[12] K.B. Hartman, D.K. Hamlin, D.S. Wilbur, L.J. Wilson, Small, 3 (2007) 1496-1499.
[13] Z. Liu, W. Cai, L. He, N. Nakayama, K. Chen, X. Sun, X. Chen, H. Dai, Nat. Nanotechnol., 2 (2006) 47.
[14] R. Singh, D. Pantarotto, L. Lacerda, G. Pastorin, C. Klumpp, M. Prato, A. Bianco, K. Kostarelos, Proc. Natl. Acad. Sci. U. S. A., 103 (2006) 3357.
[15] M.R. McDevitt, D. Chattopadhyay, B.J. Kappel, J.S. Jaggi, S.R. Schiffman, C. Antczak, J.T. Njardarson, R. Brentjens, D.A. Scheinberg, J. Nucl. Med., 48 (2007) 1180-1189.
[16] M. Prato, K. Kostarelos, A. Bianco, Accounts Chem. Res., 41 (2008) 60-68.
[17] L. Cabana, M. Bourgognon, J.T.-W. Wang, A. Protti, R. Klippstein, R.T.M. de Rosales, A.M. Shah, J. Fontcuberta, E. Tobías-Rossell, J.K. Sosabowski, K.T. Al-Jamal, G. Tobias, Small, 12 (2016) 2893-2905.
[18] S.S. Wong, E. Joselevich, A.T. Woolley, C.L. Cheung, C.M. Lieber, Nature, 394 (1998) 52.
[19] C.J. Serpell, K. Kostarelos, B.G. Davis, ACS Central Sci., 2 (2016) 190-200.
[20] L. Shao, G. Tobias, Y. Huh, M.L.H. Green, Carbon, 44 (2006) 2855-2858.
[21] M. Martincic, S. Vranic, E. Pach, S. Sandoval, B. Ballesteros, K. Kostarelos, G. Tobias, Carbon, 141 (2019) 782-793.
[22] H.-F. Cui, S.K. Vashist, K. Al-Rubeaan, J.H.T. Luong, F.-S. Sheu, Chem. Res. Toxicol., 23 (2010) 1131-1147.
[23] V.L. Colvin, Nat. Biotechnol., 21 (2003) 1166.
[24] D. Cui, F. Tian, C.S. Ozkan, M. Wang, H. Gao, Toxicol. Lett., 155 (2005) 73-85.
[25] G. Jia, H. Wang, L. Yan, X. Wang, R. Pei, T. Yan, Y. Zhao, X. Guo, Environ. Sci. Technol., 39 (2005) 1378-1383.
[26] L.P. Zanello, B. Zhao, H. Hu, R.C. Haddon, Nano Lett., 6 (2006) 562-567.
[27] K. Kostarelos, Nat. Biotechnol., 26 (2008) 774.
[28] P. Liu, Eur. Polym. J., 41 (2005) 2693-2703.
[29] V. Georgakilas, N. Tagmatarchis, D. Pantarotto, A. Bianco, J.-P. Briand, M. Prato, Chem. Commun., (2002) 3050-3051.
[30] C.J. Serpell, R.N. Rutte, K. Geraki, E. Pach, M. Martincic, M. Kierkowicz, S. De Munari, K. Wals, R. Raj, B. Ballesteros, G. Tobias, D.C. Anthony, B.G. Davis, Nat. Commun., 7 (2016) 13118.
[31] S. Daniel, T.P. Rao, K.S. Rao, S.U. Rani, G.R.K. Naidu, H.-Y. Lee, T. Kawai, Sens. Actuator B-Chem., 122 (2007) 672-682.
[32] B.K. Gorityala, J. Ma, X. Wang, P. Chen, X.-W. Liu, Chem. Soc. Rev., 39 (2010) 2925-2934.
[33] S.Y. Hong, G. Tobias, K.T. Al-Jamal, B. Ballesteros, H. Ali-Boucetta, S. Lozano-Perez, P.D. Nellist, R.B. Sim, C. Finucane, S.J. Mather, M.L.H. Green, K. Kostarelos, B.G. Davis, Nat. Mater., 9 (2010) 485.
[34] Z. Liu, X. Sun, N. Nakayama-Ratchford, H. Dai, ACS Nano, 1 (2007) 50-56.
[35] C.R. Martin, P. Kohli, Nat. Rev. Drug Discov., 2 (2003) 29.
[36] B. Ballesteros, G. Tobias, L. Shao, E. Pellicer, J. Nogués, E. Mendoza, M.L.H. Green, Small, 4 (2008) 1501-1506.
[37] M. Kierkowicz, E. Pach, A. Santidrián, S. Sandoval, G. Gonçalves, E. Tobías-Rossell, M. Kalbáč, B. Ballesteros, G. Tobias, Carbon, 139 (2018) 922-932.
[38] K. Kordatos, T. Da Ros, S. Bosi, E. Vázquez, M. Bergamin, C. Cusan, F. Pellarini, V. Tomberli, B. Baiti, D. Pantarotto, V. Georgakilas, G. Spalluto, M. Prato, J. Org. Chem., 66 (2001) 4915-4920.
[39] S. De Munari, T. Schiffner, B.G. Davis, Isr. J. Chem., 55 (2015) 387-391.
[40] B.S. Patil, V.V.S. Babu, Indian J. Chem., 43B (2004) 1288-1291.
[41] M. Bergmann, Justus Liebigs Ann. Chem. , 434 (1923) 79-110.
[42] G. Tobias, B. Ballesteros, M.L.H. Green, Phys. Status Solidi C, 7 (2010) 2739-2742.
[43] W. Wu, S. Wieckowski, G. Pastorin, M. Benincasa, C. Klumpp, J.-P. Briand, R. Gennaro, M. Prato, A. Bianco, Angew. Chem. Int. Edit., 44 (2005) 6358-6362.
[44] M. Maggini, G. Scorrano, M. Prato, J. Am. Chem. Soc., 115 (1993) 9798-9799.
[45] S.Y. Hong, G. Tobias, B. Ballesteros, F. El Oualid, J.C. Errey, K.J. Doores, A.I. Kirkland, P.D. Nellist, M.L.H. Green, B.G. Davis, J. Am. Chem. Soc., 129 (2007) 10966-10967.
[46] P. Garnier, X.-T. Wang, M.A. Robinson, S. van Kasteren, A.C. Perkins, M. Frier, A.J. Fairbanks, B.G. Davis, J. Drug Target., 18 (2010) 794-802.
[47] Y.C. Lee, C.P. Stowell, M.J. Krantz, Biochemistry, 15 (1976) 3956-3963.

[48] H. Ge, P.J. Riss, V. Mirabello, D.G. Calatayud, S.E. Flower, R.L. Arrowsmith, T.D. Fryer, Y. Hong, S. Sawiak, R.M.J. Jacobs, S.W. Botchway, R.M. Tyrrell, T.D. James, J.S. Fossey, J.R. Dilworth, F.I. Aigbirhio, S.I. Pascu, Chem, 3 (2017) 437-460.
[49] R.J. Stockert, A.G. Morell, I.H. Scheinberg, Science, 186 (1974) 365.
[50] D.K. Marsee, A. Venkateswaran, H. Tao, D. Vadysirisack, Z. Zhang, D.D. Vandre, S.M. Jhiang, J. Biol. Chem., 279 (2004) 43990-43997.

Graphical Abstract

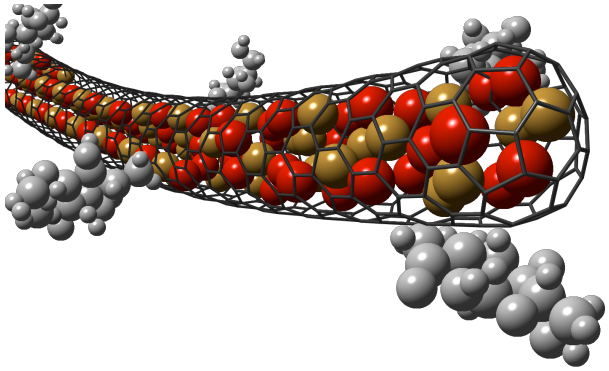

Supplementary Data (Appendix A)

In vivo behaviour of glyco-NaI@SWCNT 'nanobottles'

Sonia De Munari,[a] Stefania Sandoval,[b] Elzbieta Pach,[c] Belén Ballesteros,[c] Gerard Tobias,[b]* Daniel C. Anthony[d]* and Benjamin G. Davis[a]*

S1. GENERAL CONSIDERATIONS AND SYNTHESIS

- **Microscopic characterization**

The successful filling of SWCNTs was confirmed recording HRTEM images, high-angle annular dark field (HAADF) images in scanning transmission electron microscopy (STEM) mode and energy dispersive X-ray spectroscopy (EDX). Images and EDX data were acquired at 200 kV on a FEI Tecnai G2 F20 HR(S)TEM equipped with an EDAX super ultra-thin window (SUTW) X-ray detector. Samples were prepared dispersing a small amount in hexane and sonicating during 15 min. Afterwards, the solution was placed dropwise onto lacey carbon coated Cu support grids.

- **Thermogravimetric analysis (TGA)**

TGA was performed on a Netzsch STA 449 F1 Jupiter® instrument. Analyses were performed under flowing synthetic air at temperatures ranged between 25 ºC and 900 ºC using a heating rate of 10 ºC.min^{-1}.

- **Nuclear Magnetic Resonance and Mass spectrometry**

Proton nuclear resonance magnetic (^{1}H NMR) spectra, ^{13}C NMR, correlation spectroscopy (COSY) and heteronuclear single-quantum correlation spectroscopy (HSQC), were recorded on Bruker AV500, Bruker AV400 and Bruker AV250 (500,

400, 250 MHz) spectrometers. All chemical shifts are quoted on the δ scale in ppm, using residual solvents as the internal standard (^{1}H NMR: $CDCl_3$ = 7.26, DMSO-d_6 = 2.50, MeOD = 3.31, D_2O = 4.79; ^{13}C NMR: $CDCl_3$ = 77.16, DMSO-d_6 = 39.52, MeOD = 49.00). Coupling constants (*J*) are reported in Hz with the following splitting abbreviations: s = singlet, d = doublet, t = triplet, q = quartet, m = multiplet, dd = doublet of doublets, dt = doublet of triplets, qd = quartet of doublets, ddd = doublet of doublet of doublets, br = broad. All chemical shifts were assigned using COSY and HSQC spectra.

Low resolution mass spectra (LRMS) and high resolution MS (HRMS) were recorded on a Waters Micromass LCT Premier TOF spectrometer using electrospray ionisation (ESI).

Liquid Chromatography-Mass Spectrometry (LC-MS) was performed on a Waters LCT Premier XE (ESI-TOF-MS) coupled to a Waters 1525 Micro HPLC pump 2777 autosampler, using a Merk Chromolith RP-18 2 x 5 mm guard column. Water containing 0.1% formic acid by volume (solvent A) and acetonitrile (solvent B), were used as the mobile phase at a flow rate of 0.4 mL/min. The gradient was programmed as follows:

- 0 min 95% A 5% B 0.4 mL/min
- 1 min 95% A 5% B 0.4 mL/min
- 5 min 0% A 100% B 0.4 mL/min
- 8 min 0% A 100% B 1 mL/min
- 8.1 min 95% A 5% B 1 mL/min

The electrospray source was operated with a capillary voltage of 3 kV and a cone voltage of 100 V. Nitrogen was used as the nebulizer and desolvation gas, at a total flow of 300 L/hr.

- **General Synthetic Methods**

Thin layer chromatography (TLC) was carried out using Merck aluminium backed sheets coated with 60 F254 silica gel. Visualisation of the silica plates was achieved using a UV lamp (λmax = 254 nm), and/or ammonium molybdate (5% in 2 M H_2SO_4), ninhydrin (1.5 g ninhydrin, 5 mL acetic acid, 500 mL 95% ethanol) or sulfuric acid (45 mL methanol, 45 mL water, 3 mL sulfuric acid) solutions. Flash column chromatography was carried out using Geduran Si 60 (40-63 μm) Merk. Mobile phases are reported as ratio volume:volume.

All solvents were used as supplied (analytical or HPLC grade), without prior purification. PE refers to the fraction of petroleum ether boiling in the range of 40-60 °C. All reactions requiring anhydrous conditions we performed inflame-dried flasks, with activated molecular sieves, dried solvents and argon atmosphere. Brine refers to a saturated aqueous solution of sodium chloride. Anhydrous magnesium sulphate ($MgSO_4$) was used as drying agent after reaction work-up. Deionised water was used for chemical reactions and protein manipulations. Reagents were purchased from Sigma-Aldrich and used as supplied.

Nanotubes were purified and filled in a Carbolite horizontal single zone tube furnace, model MTF 12/38/250 with PID controller type 3216P1. Radioactive samples were counted on a Autogamma counter (Packard Instrument Co., Downers Grove, IL). Elemental analyses were run by Stephen Boyer (Science Centre, London Metropolitan University, 29 Hornsey Road, London N7 7DD).

Animals were purchased from Charles River (UK); animal experiments were performed by Sonia De Munari (PIL: IC7F41F8D) and Daniel Anthony under project license 30/3076 with the UK Home Office and local ethical approval.

Room temperature was defined as 21 °C.

- **Synthesis of f-NaI@SWCNTs**

4-(2-(bis(2-aminoethyl)amino)ethylamino)oxobutanoic acid :**TLC** R_f = 0.1 (WIPE, 1:2:2); **^{1}H NMR** (MeOD, 400 MHz) δ 3.30 (t, *J* = 4.6 Hz, 2 H, C**H_2**NH) , 2.86 (t, *J* = 4.6 Hz, 4 H, 2 x C**H_2**NH_2), 2.64-2.59 (t, *J* = 4.5 Hz, 6 H, 3 x CH_2N), 2.45 (br, 4 H, $COCH_2CH_2CO$); **^{13}C NMR** (MeOD, 101 MHz) δ 175.10, 179.93 (2 x CO), 54.25, 55.12 (3 x CH_2N), 38.28, 38.53 (CH_2NH, 2 x CH_2NH_2), 32.75, 33.35 (CO**C**H_2**C**H_2CO); **LRMS** (ESI^+) m/z = 247.31 [M+H]; **HRMS** (ESI^+) found 247.1763 [M+H], $C_{10}H_{23}N_4O_3$ requires 247.1765; **IR** (ATR) 3271.00 (OH), 1703.87 (COOH), 1697.90 (CONH).

4-(2-(bis(2-tert-butoxycarbonyl-aminoethyl)amino)ethylamino)oxobutanoic acid: **TLC** R_f = 0.85 (DCM:MeOH, 10:1); **^{1}H NMR** ($CDCl_3$, 250 MHz) δ 3.27 (br, 2 H, C**H_2**$NHCOCH_2$), 3.13 (br, 4 H, 2 x C**H_2**NHCOO) , 2.52 (br, 10 H, 3 x CH_2N, $COCH_2CH_2CO$), 1.41 (s, 18 H, 2 x ^{t}Bu); **^{13}C NMR** ($CDCl_3$, 126 MHz) δ 172.69, 157.98, (2 x **C**OCH_2), 156.63 (2 x **C**OOC), 81.28 (**C**$(CH_3)_3$), 79.46, 79.22 (3 x CH_2N), 39.10, 36.86 (3 x CH_2NH), 31.66, 31.02 (CO**C**H_2**C**H_2CO), 28.40 (C(**C**$H_3)_3$); **LRMS** (ESI^+) m/z = 447.55 [M+H]; **HRMS** (ESI^+) found 447.2819 [M+H], $C_{20}H_{39}N_4O_7$ requires 447.2813; **IR** (ATR) 3277.19 (OH), 1708.15 (COOH), 1699.62 (CONH), 1692.96 (COOC); **m.p.** = 58-61 °C.

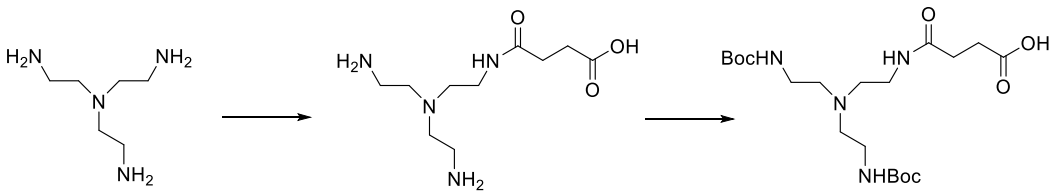

N-(2,2'-(ethylenedioxy)diethylamino) benzylacetate: **TLC** R_f = 0.0 (EtOAc, 100%); **^{1}H NMR** ($CDCl_3$, 500 MHz) δ 7.35-7.24 (br, 5 H, CH-Ar), 5.15 (br, 2 H, CH_2Ph), 3.93 (br, 2 H, NHC**H_2**CO), 3.72 (br, 2 H, OCH_2C**H_2**NH_2), 3.66 (br, 2 H, CH_2C**H_2**NH), 3.59 (br, 4

H, OCH_2CH_2O), 3.31 (br, 2 H, $OC\mathbf{H_2}CH_2NH$), 3.22 (br, 2 H, $OC\mathbf{H_2}CH_2NH_2$); **^{13}C NMR** ($CDCl_3$, 126 MHz) δ 166.16 (CO), 133.83 (C-Ar), 118.77, 116.48, 114.19, 111.91 (5 x CH-Ar), 69.73, 69.85 (OCH_2CH_2O), 68.78 ($COO\mathbf{C}H_2Ar$), 64.99, 65.73 (2 x $O\mathbf{C}H_2CH_2N$), 47.89 ($NH\mathbf{C}H_2CO$), 47.76 ($CH_2\mathbf{C}H_2NH$), 40.10 (CH_2NH_2); **LRMS** (ESI^+) m/z = 297.37 [M+H]; **HRMS** (ESI^+) found 297.1811 [M+H], $C_{15}H_{25}N_2O_4$ requires 297.1809; **IR** (ATR) 3274.78 (NH_2), 1619.62 (CO), 720.61 (arom).

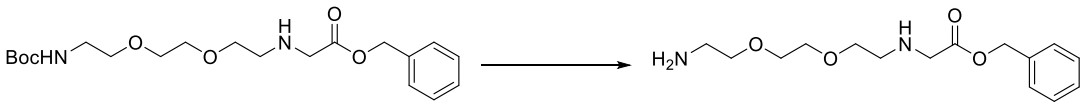

N-(4-(2-(bis(2-tert-butoxycarbonyl-aminoethyl)amino)ethylamino)oxobutanoyl) N-(2,2'-ethylenedioxy)diethylamino)benzylic acid: **(1) TLC** R_f = 0.55 (DCM:MeOH, 9:1); **^{1}H NMR** (DMSO-d_6, 400 MHz) δ 7.86 (s, 1 H, NH), 7.46-7.31 (br, 5 H, CH-Ar), 6.79 (s, 1 H, NH), 5.23 (s, 2 H, CH_2Ph), 4.02 (s, 2 H, $COC\mathbf{H_2}NH$), 3.73-3.64 (t, *J* = 4.6 Hz, 2 H, $OCH_2C\mathbf{H_2}NHCO$), 3.53 (dt, *J* = 7.9, 4.8 Hz, 6 H, $OC\mathbf{H_2}C\mathbf{H_2}O$, $OCH_2C\mathbf{H_2}NHCH_2$), 3.38 (t, *J* = 6.0 Hz, 2 H, $OC\mathbf{H_2}CH_2NHCH_2$), 3.25-3.07 (br, 6 H, $COCH_2CH_2CO$, $NCH_2C\mathbf{H_2}NHCOCH_2$), 3.02 (t, *J* = 4.6 Hz, 2 H, $NC\mathbf{H_2}CH_2NHCOCH_2$), 2.60 (t, *J* = 4.6 Hz, 4 H, $NC\mathbf{H_2}CH_2NHCOO$), 2.31 (br, 4 H, 2 x $C\mathbf{H_2}NHCOO$), 1.37 (s, 18 H, 2 x ^{t}Bu); **^{13}C NMR** (DMSO-d_6, 101 MHz) δ 171.98 ($\mathbf{C}OCH_2CH_2\mathbf{C}O$), 167.62 ($CH_2\mathbf{C}OO$), 156.15 (2 x NHCOO), 135.69 (C-Ar), 128.95, 128.85, 128.72 (5 x CH-Ar), 78.22 ($\mathbf{C}(CH_3)_3$), 70.03 (OCH_2CH_2O), 69.82 ($OCH_2\mathbf{C}H_2NHCH_2$), 69.53 ($O\mathbf{C}H_2CH_2NHCH_2$), 67.25 (CH_2Ph), 66.44 ($OCH_2\mathbf{C}H_2NHCOCH_2$), 53.86 ($N\mathbf{C}H_2CH_2NHCOO$), 47.69 ($NH\mathbf{C}H_2CO$), 46.87 ($NCH_2\mathbf{C}H_2NHCOCH_2$), 38.94 ($CO\mathbf{C}H_2\mathbf{C}H_2CO$), 37.94 ($N\mathbf{C}H_2CH_2NHCOCH_2$), 31.06 ($NCH_2\mathbf{C}H_2NHCOO$), 28.67 ($C(\mathbf{C}H_3)_3$); **LRMS** ($ESI^+$) m/z = 725.89 [M+H]; **HRMS** (ESI^+) found 725.4439 [M+H], $C_{35}H_{61}N_6O_{10}$ requires

725.4444; **IR** (ATR) 3307.05 (NH), 2975.23 (CH), 1693.88 (CONH), 1650.52 ($COCH_2Ph$), 719.16 (arom).

(2) TLC R_f = 0.0 (DCM:MeOH, 8:2); **^{1}H NMR** (DMSO-d_6, 400 MHz) δ 7.98 (d, *J* = 5.8 Hz, 1 H, NH), 6.85 (s, 1 H, NH), 3.80-3.62 (t, *J* = 4.6 Hz, 4 H, $OC\mathbf{H_2}CH_2NHCOCH_2$, $OC\mathbf{H_2}CH_2NHCH_2$), 3.60-3.46 (br, 6 H, OCH_2CH_2O, $OCH_2C\mathbf{H_2}NHCH_2$), 3.39 (t, *J* = 5.8 Hz, 2 H, $OCH_2C\mathbf{H_2}NHCOCH_2$), 3.19 (t, *J* = 4.6 Hz, 4 H, $COCH_2CH_2CO$), 3.15-3.09 (t, *J* = 4.6 Hz, 2 H, $NHC\mathbf{H_2}COOH$), 3.06 (t, *J* = 4.6 Hz, 4 H, $NC\mathbf{H_2}C\mathbf{H_2}NHCOCH_2$), 2.72 (t, *J* = 4.6 Hz, 4 H, 2 x $NC\mathbf{H_2}CH_2NHCOO$), 2.31 (t, *J* = 4.6 Hz, 4 H, 2 x $NCH_2C\mathbf{H_2}NHCOO$), 1.37 (s, 18 H, 2 x ^{t}Bu); **^{13}C NMR** (DMSO-d_6, 101 MHz) δ 180.63 (COOH), 172.15, 171.99 (2 x $\mathbf{C}OCH_2$), 156.15 (2 x NHCOO), 78.33 ($\mathbf{C}(CH_3)_3$), 72.82 (OCH_2CH_2O), 69.83 ($OCH_2\mathbf{C}H_2NHCH_2$), 69.56 ($O\mathbf{C}H_2CH_2NHCH_2$), 66.17 ($OCH_2\mathbf{C}H_2NHCOCH_2$), 53.34 ($N\mathbf{C}H_2CH_2NHCOO$), 47.83 ($NH\mathbf{C}H_2COOH$), 46.44 ($NCH_2\mathbf{C}H_2NHCOCH_2$), 38.92 ($CO\mathbf{C}H_2\mathbf{C}H_2CO$), 36.22 ($N\mathbf{C}H_2CH_2NHCOCH_2$), 31.08 ($NCH_2\mathbf{C}H_2NHCOO$), 28.67 ($C(\mathbf{C}H_3)_3$); **LRMS** ($ESI^-$) m/z = 633.76 [M-H]; **HRMS** (ESI^-) found 633.3833 [M-H], $C_{28}H_{53}N_6O_{10}$ requires 633.3829; **IR** (ATR) 3342.83 (NH), 1634.52 (CONH), 1700.11 (COOH).

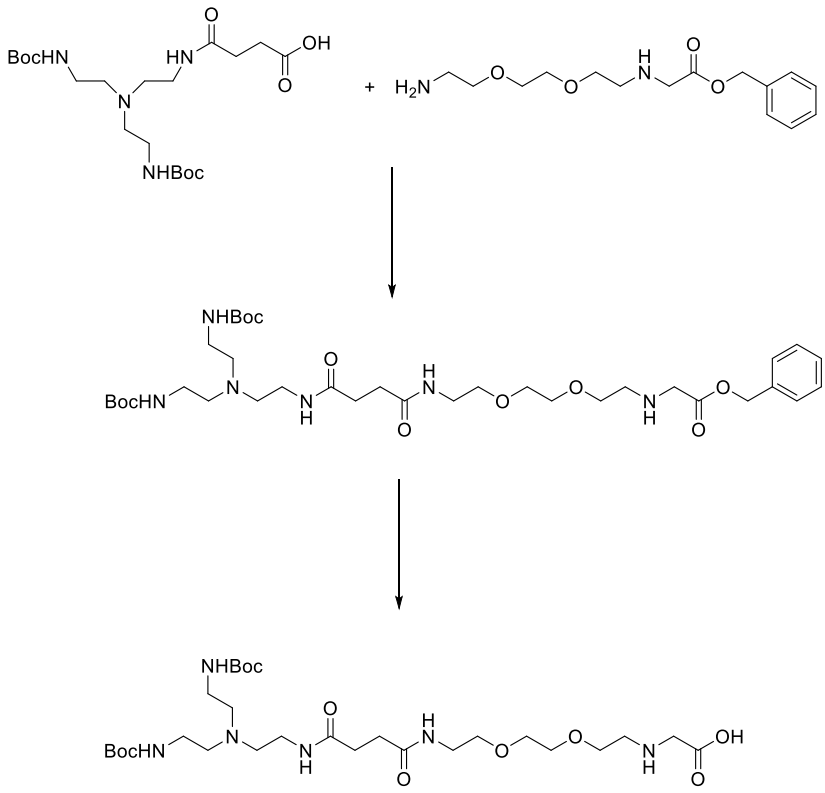

1.0

- **– Synthesis of Glycosylated-NaI@SWCNTs**

2-acetamido-1-thio-(S-2-imido-2-methoxyethyl)-2-deoxy-β-D-glucopyranoside: **TLC** R_f = 0.0 (DCM:MeOH, 10:1); **^{1}H NMR** (D_2O, 500 MHz) δ 4.71 (d, *J* = 9.3 Hz, 1 H, H-1), 3.85 (dd, *J* = 12.4, 2.0 Hz, 1 H, H-6a), 3.72 (t, *J* = 10.1 Hz, 1 H, H-2), 3.67 (dd, *J* = 12.4, 5.4 Hz, 1 H, H-6b), 3.56-3.47 (t, *J* = 10.1 Hz, 1 H, H-3), 3.46-3.34 (br, 4 H, C**H$_2$**CNH, H-5, H-4), 3.26 (s, 3 H, OMe), 1.95 (s, 3 H, Ac); **^{13}C NMR** (D_2O, 126 MHz) δ 174.66 (CO),118.43 (CN), 83.80 (C-1), 80.29 (C-5), 75.08 (C-3), 69.99 (C-4), 60.92, 60.89 (C-6, **C**H_2CNH), 54.34 (C-2), 48.83 (OMe), 22.07 (Ac).

1,2,3,6-O-tetra-O-acetyl-4-O-[2,3,4,6-tetra-O-acetyl-β-D-galactopyranosyl]-β-D-glucopyranoside **TLC** R_f = 0.2 (PE:EtOAc, 1:1); **^{1}H NMR** ($CDCl_3$, 400 MHz) δ 6.23 (d, *J* = 3.7 Hz, 0.3 H, H-1eq), 5.65 (d, *J* = 8.3 Hz, 0.7 H, H-1ax), 5.48-5.41 (t, *J* = 9.2 Hz, 0.3 H, H-3α), 5.34 (t, *J* = 3.2 Hz, 1 H, H-4'), 5.23 (t, *J* = 9.2 Hz, 0.7 H, H-3β), 5.14 (t,

J = 9.5 Hz, 1 H, H-4), 4.91 (dd, *J* = 10.4, 7.9 Hz, 1 H, H-2'), 4.89 (dd, *J* = 10.0, 4.0 Hz, 1 H, H-2), 4.51 (ddd, *J* = 9.9, 5.0, 1.9 Hz, 1 H, H-5), 4.38 (t, *J* = 6.8 Hz, 1 H, H-5'), 4.17 (dd, *J* = 12.1, 1.9 Hz, 1 H, H-6a), 4.02 (dd, *J* = 12.1, 1.9 Hz, 1 H, H-6'a), 3.92 (dd, *J* = 12.1, 1.9 Hz, 1 H, H-6b), 3.70 (dd, *J* = 12.1, 1.9 Hz, 1 H, H-6'b), 2.21, 2.14, 2.10, 2.08, 2.05, 2.03, 2.01, 1.95 (8 x s, 8 x 3 H, 8 x OAc); **^{13}C NMR** ($CDCl_3$, 101 MHz) δ 170.76, 170.72, 170.54, 170.38, 170.27, 170.11, 169.84, 168.52 (8 x CO), 101.37 (C-1'), 87.22 (C-1), 74.33 (C-4), 72.35 (C-5), 71.52 (C-3'), 70.34 (C-5'), 70.11 (C-2), 69.34 (C-3), 69.12 (C-2'), 67.32 (C-4'), 60.92 (C-6'), 60.34 (C-6), 20.97, 20.88, 20.76, 20.71, 20.69, 20.65, 20.53, 20.12 (8 x Ac); **LRMS** (ESI^+) m/z = 679 [M+H]; $[\alpha]_D^{20}$ = + 32.9 (c = 1, $CHCl_3$), + 30.2 (c = 1, $CHCl_3$); [1] **IR** (ATR) 1744 (CO); **m.p.** = 131-134 °C, lit 135 °C.[1]

2,3,6-O-tri-O-acetyl-4-O-[2,3,4,6-tetra-O-acetyl-β-D-galactopyranosyl]-1-bromo-α-D-glucopyranoside: **TLC** R_f = 0.3 (PE:EtOAc, 1:1); **^{1}H NMR** ($CDCl_3$, 400 MHz) δ 6.50 (d, *J* = 4.0 Hz, 1 H, H-1), 5.52 (t, *J* = 9.6 Hz, 1 H, H-3), 5.33 (d, *J* = 2.9 Hz, 1 H, H-4'), 5.10 (dd, *J* = 10.4, 7.9 Hz, 1 H, H-2'), 4.93 (dd, *J* = 10.4, 3.4 Hz, 1 H, H-3'), 4.73 (dd, *J* = 10.0, 4.0 Hz, 1 H, H-2), 4.49 (d, *J* = 7.9 Hz, 2 H, H-1', H-6a), 4.29 (d, *J* = 7.9 Hz, 2 H, H-1', H-6b), 3.97 (dd, *J* = 12.1, 1.9 Hz, 2 H, H-6'), 3.97 (ddd, *J* = 9.9, 5.0, 1.9 Hz, 1 H, H-5), 3.93 (t, *J* = 6.8 Hz, 1 H, H-5'), 3.76 (t, *J* = 9.5 Hz, 1 H, H-4), 2.13, 2.11, 2.07, 2.04, 2.04, 2.03, 1.94 (7 x s, 7 x 3 H, 7 x OAc); **^{13}C NMR** ($CDCl_3$, 101 MHz) δ 170.37, 170.20, 170.17, 170.10, 170.00, 169.26, 168.98 (7 x CO), 100.83 (C-1'), 86.43 (C-1), 74.98 (C-4), 72.99 (C-5), 71.00 (C-3'), 70.85 (C-5'), 70.78 (C-2), 69.59 (C-3), 69.01 (C-2'), 66.62 (C-4'), 61.06 (C-6'), 60.90 (C-6), 20.84, 20.81, 20.74, 20.69, 20.68, 20.858, 20.53 (7 x Ac); **LRMS** (ESI^+) m/z = 700 [M+H]; $[\alpha]_D^{20}$ = - 103.1

(c = 1, $CHCl_3$), lit - 102.0 (c = 1, $CHCl_3$) [2]; **IR** (ATR) 1743 (CO); **m.p.** = 128-131 °C, lit 135 °C.[2]

2,3,6-O-tri-O-acetyl-4-O-[2,3,4,6-tetra-O-acetyl-β-D-galactopyranosyl]-1-thio-(S-cyanomethyl)-β-D-glucopyranoside : **TLC** R_f = 0.25 (PE:EtOAc, 1:1); **^{1}H NMR** ($CDCl_3$, 400 MHz) δ 5.34 (d, *J* = 2.6 Hz, 1 H, H-4'), 5.24 (t, *J* = 9.2 Hz, 1 H, H-3), 5.10 (dd, *J* = 10.4, 7.9 Hz, 1 H, H-2'), 5.02 (dd, *J* = 10.0, 4.0 Hz, 1 H, H-2), 4.88 (dd, *J* = 10.4, 3.4 Hz, 1 H, H-3'), 4.68 (d, *J* = 10.0 Hz, 1 H, H-1), 4.54 (dd, *J* = 12.1, 1.9 Hz, 1 H, H-6a), 4.48 (d, *J* = 7.9 Hz, 1 H, H-1'), 4.19 (dd, *J* = 12.1, 1.9 Hz, 1 H, H-6b), 4.02 (dd, *J* = 12.1, 1.9 Hz, 2 H, H-6'), 3.87 (t, *J* = 6.8 Hz, 1 H, H-5'), 3.82 (t, *J* = 9.5 Hz, 1 H, H-4), 3.68 (ddd, *J* = 9.9, 5.0, 1.9 Hz, 1 H, H-5), 3.58 (d, *J* = 17.0 Hz, 1 H, CH_2aCN), 3.29 (d, *J* = 17.0 Hz, 1 H, CH_2bCN), 2.14, 2.12, 2.09, 2.06, 2.06, 2.04, 1.95 (7 x s, 7 x 3 H, 7 x OAc); **^{13}C NMR** ($CDCl_3$, 101 MHz) δ 170.38, 170.16, 170.10, 169.81, 169.57, 169.32, 169.03 (7 x CO), 115.74 (CN), 101.06 (C-1'), 81.48 (C-1), 75.79 (C-5), 73.25 (C-4), 70.94 (C-3), 70.78 (C-5'), 69.89, 69.87 (C-3', C-2), 69.04 (C-2'), 66.61 (C-4'), 61.63 (C-6'), 60.83 (C-6), 20.87, 20.81, 20.76, 20.71, 20.68, 20.65, 20.54 (7 x OAc), 14.48 (**C**H_2CN); **LRMS** (ESI^+) m/z = 692 [M+H]; **HRMS** (ESI^+) found 692.1887 [M+H], $C_{28}H_{38}NO_{17}S$ requires 692.1855; $[\alpha]_D^{20}$ = + 34.1 (c = 1, $CHCl_3$); **IR** (ATR) 22141 (CN), 1743 (CO); **m.p.** = 180-185 °C.

4-O-[β-D-galactopyranosyl]-1-thio-(S-2-imido-2-methoxyethyl)-β-D-glucopyranoside: **TLC** R_f = 0.0 (DCM:MeOH, 10:1). **^{1}H NMR** (D_2O, 500 MHz) δ 4.51 (d, *J* = 9.9 Hz, 1 H, H-1), 4.37 (d, *J* = 7.8 Hz, 1 H, H-1'), 3.87-3.82 (br, 2 H, H-6a, H-4'), 3.70 (ddd, *J* = 11.6, 8.8, 3.9 Hz, 4 H, H-6', H-6b, CH_2aCNH), 3.66-3.61 (br, 3 H, CH_2bCNH, H-3, H-5), 3.61-3.55 (br, 3 H, H-5', H-4, H-3'), 3.48-3.44 (br, 1 H, H-2'), 3.36-3.30 (br, 1 H, H-2), 3.26 (s, 3 H, OMe); **^{13}C NMR** (D_2O, 126 MHz) δ 175.53 (CNH), 118.56 (CN),

102.81 (C-1'), 84.87 (C-1), 78.68 (C-3), 77.82 (C-3'), 77.75, 75.61, 75.32, 72.47 (C-4, C-4', C-5, C-5'), 71.83 (C-2'), 70.91 (C-2), 68.52 (**C**H_2CNH), 61.01 (C-6), 59.98 (C-6'), 48.82 (OMe).

- **– Elemental Analysis**

f-NaI@SWCNTs: (C, H, N) 65.66, 1.13, 2.93.
GlcNAc-NaI@SWCNTs: (C, H, N) 66.81, 1.14, 3.07.

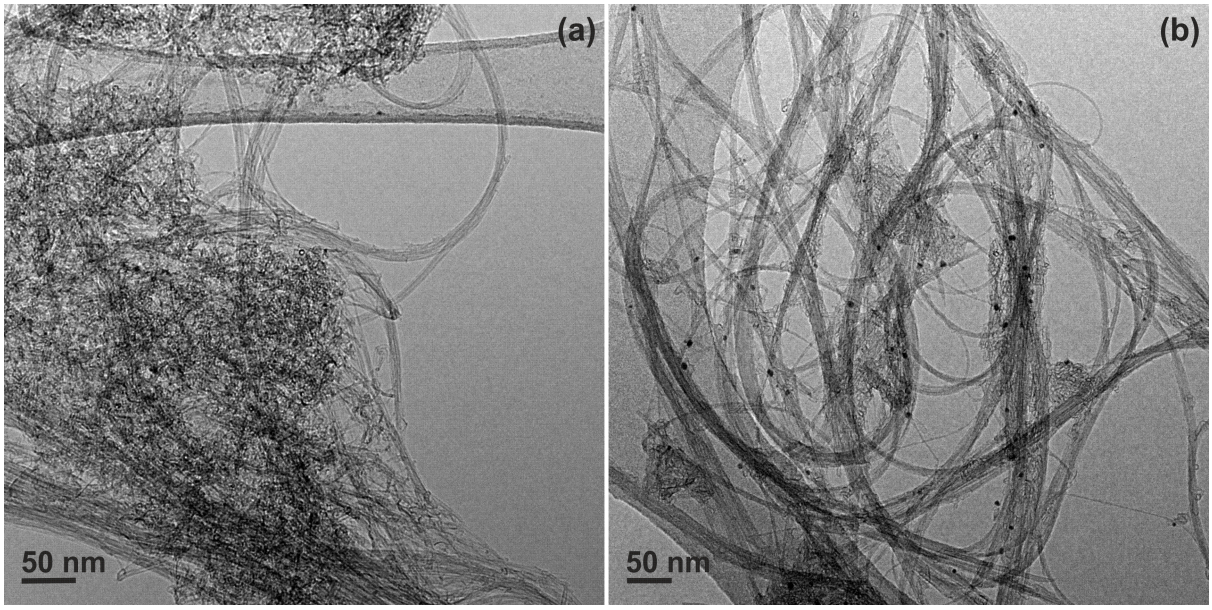

Figure S1. TEM images of bundles of (a) as-received and (b) steam purified SWCNTs. Residual Fe particles are visible as black dots.

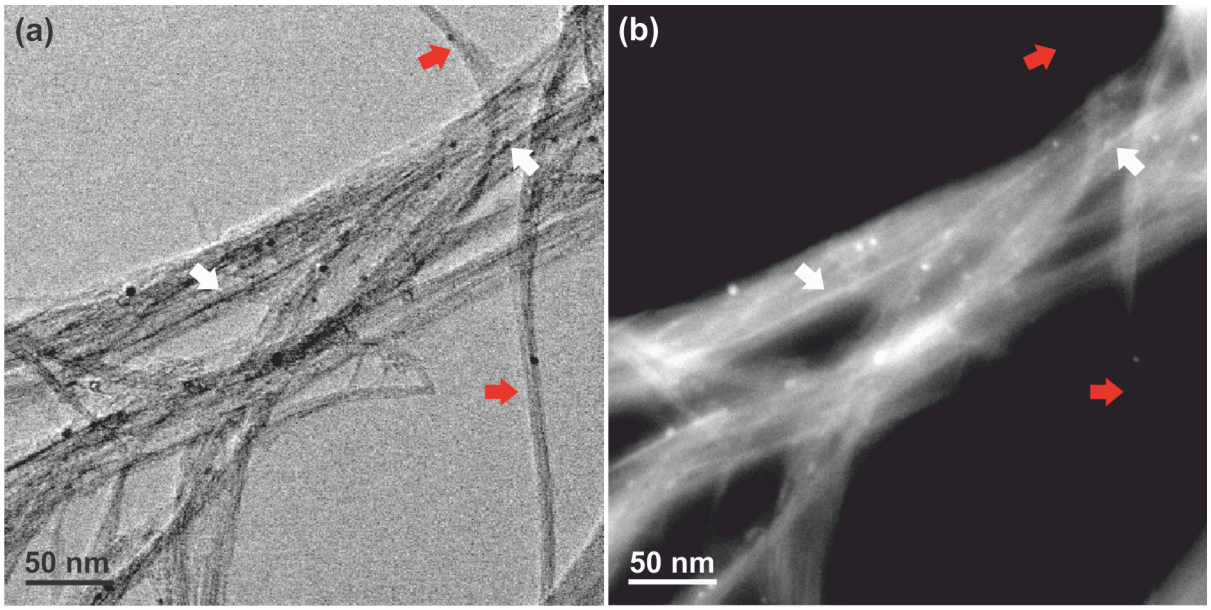

Figure S2. (a) HRTEM image of bundles of steam-purified SWCNTs filled with NaI via molten-phase capillary wetting through heating treatment up to 900 ºC. (b) HAADF-STEM image showing the contrast between the heavy atoms of the salt and C atoms. As a guide to the eye, white arrows point to filled SWCNTs and red arrows to empty SWCNTs. The visible small dots were already present in empty nanotubes and, correspond to residues from the iron-based catalyst used to generate SWNTs and that is not removed during purification.

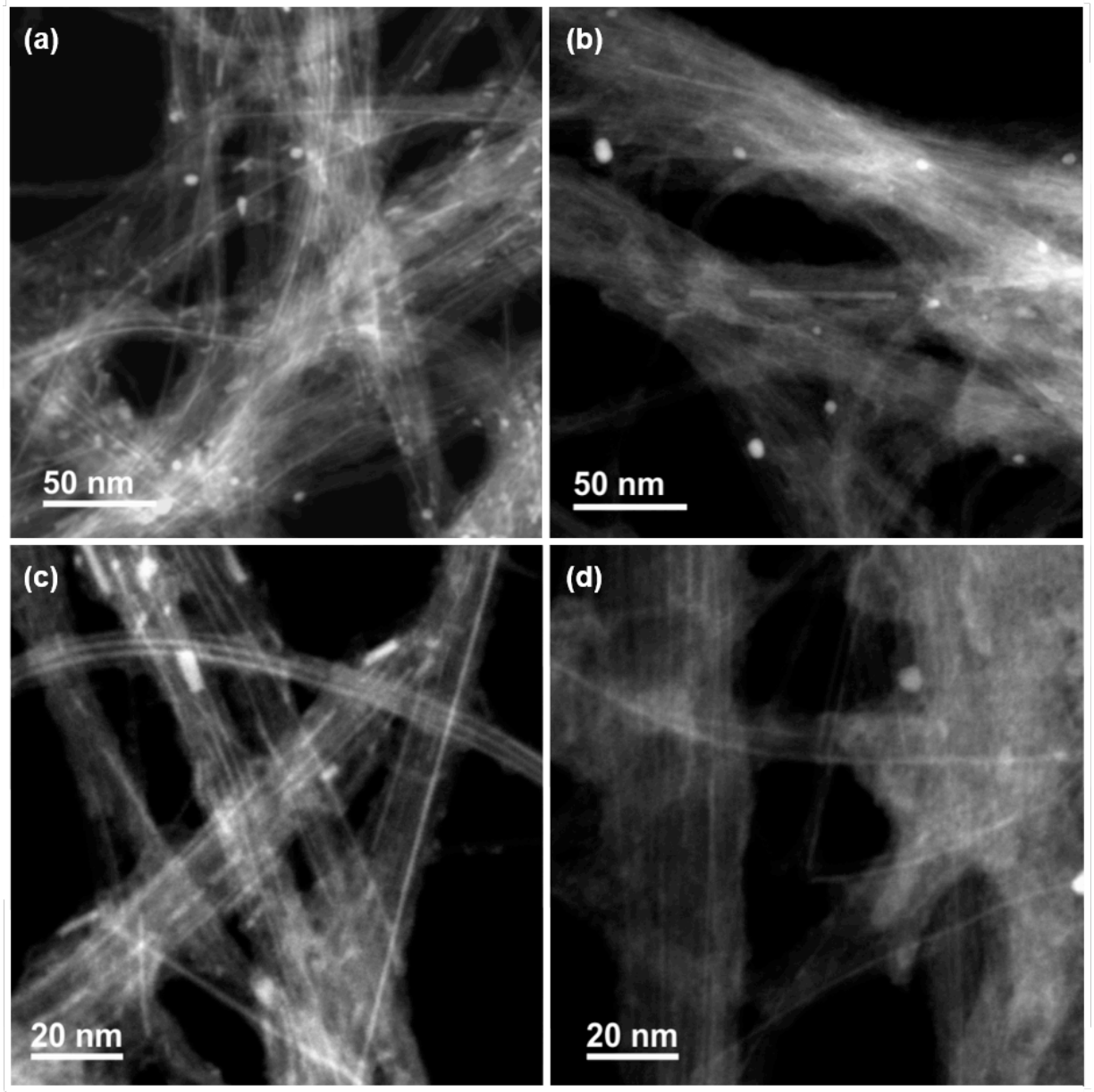

Figure S3. Additional HAADF-STEM images showing that a higher intensity in the bundle area for the GlcNAc functionalized NaI@SWCNTs (b, d) as compared to the NaI@SWCNTs (a, c).

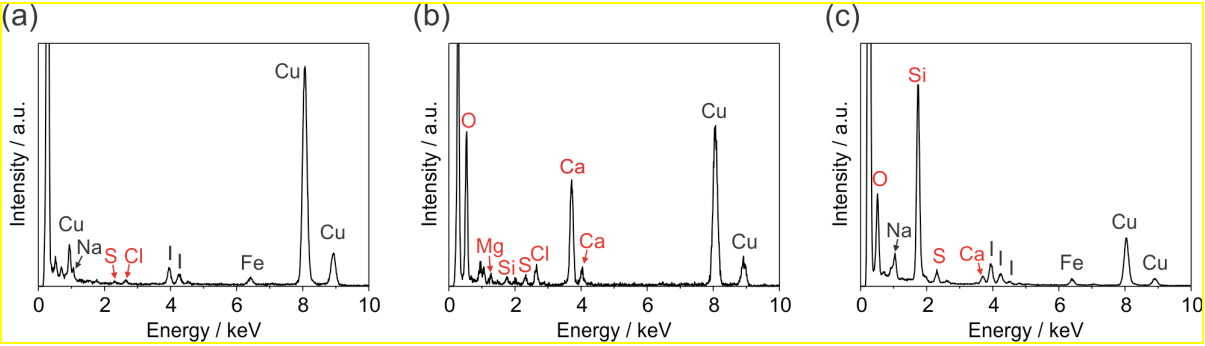

Figure S4. EDX analyses of samples (a) *f*-NaI@SWCNT, (b) $[Lac]_2$-NaI@SWCNT and (c) $[GlcNAc]_2$-NaI@SWCNT showing that some inorganic materials used during functionalization reactions and work up are retained in samples (elements in black: attributed to NaI filled carbon nanotubes; elements in red: retained due to the functionalization protocols). Cu arises from the TEM support grid.

S2. BIODISTRIBUTION STUDIES

– Gamma counting

CD-1 male mice (20-25 g body weight) were injected *i.v.* with ~0.1 mg (~ 1 MBq) of Glycosylated-Na^{125}I@SWCNTs in 100 µL of saline solution (0.9% NaCl in H_2O), under anaesthesia by isoflurane. The animals were left to recover. After 1 h mice were killed by CO_2 asphyxiation. Sections of liver (Li), lungs (Lu), heart (H), spleen (S), kidneys (K), gut (G), muscles (M1 from hind leg and M2 from front leg) and brain (B) were harvested for *ex vivo* gamma counting. All were run in triplicate.

Table S1. Activity measured by ɣ counter of organs harvested from CD-1 mice after injection of GlcNAc-Na^{125}I@SWCNTs and Lac-Na^{125}I@SWCNTs. The values are expressed as percentage of the injected dose per gram of tissue (%ID/g).

Organ	GlcNAc-Na^{125}I@SWCNTs	Lac-Na^{125}I@SWCNTs
liver	2	2
lungs	85	84
kidneys	2	2
spleen	3	2
gut	2	2
muscle 1	2	2
muscle 2	1	2
heart	1	2
brain	1	1

– ICP-MS

Samples were generated in an essentially similar manner as for gamma counter and iodine concentration measured using a Thermo Finnigan Element 2 ICP-MS (by the ICP-MS service at Oxford Earth Sciences). Calibrations were obtained using external standards (a series of standards of known iodine concentrations were prepared and analysed to gain a linear calibration linear, prior to the measurement of samples, r^2

>0.999); the required serials dilutions were made from a 1000ppm iodide standard-bought from High Purity Standards Ltd. As external quality control, an external standard was diluted and measured from a different 1000ppm iodide standard, also purchased from High Purity Standards. As a mode of internal standardization, all blanks, standards and samples were also spiked with 1ng/g Te, so that any general instrument drift could be normalised. Samples, blanks, standards and QC were diluted using a 2%HNO_3 that was adjusted to pH 9 with an addition of 3%NH_4OH reagent. All data results was measured as elemental concentrations and corrected for dilution during sample preparation; they were measured from m/z 127. The instrument detection limit was determined to be 12.9 pg/g. The method detection limit was determined to be 24.4 ng/g.

REFERENCES

[1] B.S. Patil, V.V.S. Babu, Indian J. Chem., 43B (2004) 1288-1291.

[2] Z. Zhang, G. Magnusson, Carbohydr. Res., 295 (1996) 41-55.